Rapid Communications

Electron-electron interactions in the two-dimensional semiconductor InSe

Arvind Shankar Kumar,[1,*] Kasun Premasiri,[1,*] Min Gao,[1] U. Rajesh Kumar,[2] Raman Sankar,[2,3]
Fang-Cheng Chou,[2] and Xuan P. A. Gao[1,†]
[1]*Department of Physics, Case Western Reserve University, 2076 Adelbert Road, Cleveland, Ohio 44106, USA*
[2]*Center for Condensed Matter Sciences, National Taiwan University, Taipei 10617, Taiwan*
[3]*Institute of Physics, Academia Sinica, Taipei 11529, Taiwan*

(Received 22 April 2020; revised 23 July 2020; accepted 17 August 2020; published 1 September 2020)

Electron-electron interactions (EEIs) in 2D van der Waals (vdW) nanostructures is a topic of high current interest, with implications in both fundamental physics and nanoelectronics. In this Rapid Communication, we report the observation of a negative parabolic magnetoresistance (MR) in the multilayer 2D semiconductor InSe beyond the low-field weak localization/antilocalization regime, and provide evidence for the EEI origin of this MR behavior. Further, we analyze this negative parabolic MR and other observed quantum transport signatures of EEIs (temperature-dependent conductance and Hall coefficient) within the framework of Fermi-liquid theory and extract the gate voltage tunable Fermi-liquid parameter F_0^σ which quantifies the electron spin-exchange interaction strength. This work opens up different directions for investigations of EEI effects in the electron transport of 2D vdW nanostructures.

DOI: 10.1103/PhysRevB.102.121301

Two-dimensional (2D) van der Waals (vdW) materials offer a versatile platform to venture into new facets of physics, wherein the discovery of exfoliable graphene has been the initial impetus [1–3]. Having a multitude of material candidates with exotic properties that are important in various fields such as topological phases [4–7], spintronics [8–10], and valleytronics [11], 2D materials continue to fascinate researchers with unique perspectives. In terms of electron quantum transport, 2D materials provide researchers with a diverse set of materials that can be used to obtain confined 2D electron gas (2DEG) beyond conventional semiconductor heterostructure systems [12–15]. Quantum transport studies of 2D materials have already shown great promise in various fronts ranging from exploring spin polarization effects and the underlying mechanisms to topological superconductivity and beyond [6–8,16].

Deepening the understanding of electron localization and electron-electron interactions (EEIs) has been one of the major focuses in the studies of disordered 2DEG [17–36]. Most of these studies are based on conventional semiconductors such as GaAs heterostructures [21–26], Si metal-oxide-semiconductor field-effect transistors (MOSFETs) [27–30], and, more recently, graphene [31–33]. The availability and development of new 2D materials in the past few years have opened up the opportunity to study electron quantum transport effects in new materials and/or in different transport regimes. For instance, there have been reports on weak localization (WL), weak antilocalization (WAL), and spin-orbit coupling effects in 2D semiconductors including transition-metal dichalcogenides as well as non-transition-metal chalcogenides [8,10,37].

However, a direct observation of EEIs in vdW 2D semiconductors is lacking in the literature. Probing the EEIs in new 2D materials is compelling due to the diverse set of material choices and electronic band structures to explore, compared to conventional heterointerfaces based on group IV or III-V semiconductors. To this end, we conduct a comprehensive electron transport study of the 2D semiconductor indium monoselenide (InSe) and report here various signatures of EEIs—a negative parabolic MR, and logarithmic temperature (T)-dependent Hall coefficient and conductivity [36]. Analyzing these observations within the framework of Fermi-liquid (FL) theory in the diffusive transport regime, we are able to extract the interaction parameter F_0^σ over the range of electron density $n = 3 - 8 \times 10^{12}/\text{cm}^2$ for InSe, and compare it with the predictions of FL theory.

InSe is a group-III monochalcogenide semiconductor. Se-In-In-Se atoms form individual vdW layers with a honeycomb lattice structure [15,37,38]. It has drawn a lot of attention due to its relatively high electron mobility among 2D semiconductors [15,38], strong spin-orbit coupling [37], and optoelectronic properties associated with a direct-indirect gap transition as the thickness is reduced [15,39–42]. For this study, InSe nanoflake devices were fabricated on degenerately doped Si substrates with 290 nm SiO_2 (sample 1) or 150 nm Si_3N_4 (sample 2) as the gate dielectric. β-InSe nanoflakes were mechanically exfoliated onto cleaned substrates and Ti/Ni contacts to the freshly exfoliated flakes were fabricated using stencil lithography with copper grid shadow masks, and electron-beam metal deposition.

The inset of Fig. 1(a) illustrates the device structure and van der Pauw geometry used for the transport experiments. Gold wires (50 μm in diameter) were attached to Ti/Ni

*These authors contributed equally to this work.
†Corresponding author: xuan.gao@case.edu

 ©2020 American Physical Society

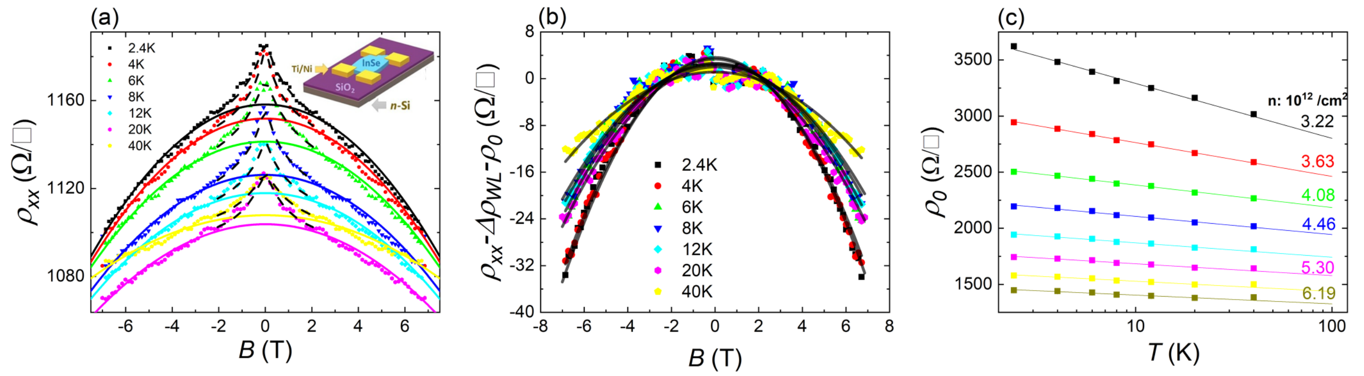

FIG. 1. (a) Magnetoresistance of InSe nanoflake sample 1 at different temperatures, plotted for $n = 6.19\times10^{12}/\,\mathrm{cm}^2$. The dotted lines correspond to fittings to the 2D weak localization (WL) effect. The solid lines correspond to fits to parabolas at high fields ($B > 2T$). Inset: Device schematic. (b) Magnetoresistance with WL correction subtracted, for data in (a). Black solid lines correspond to parabolic fits. (c) ρ_0, which is the B 0 intercept of parabolic fits shown in (a), plotted vs temperature, at different electron densities.

metal contacts using indium soldering, and then mounted onto the sample holder of a physical property measurement system (Quantum Design, Model 6000) and measured with low-frequency lock-in techniques. Longitudinal resistivity ρ_{xx} and transverse resistivity ρ_{xy} were calculated using the van der Pauw method [43], followed by symmetrization of the ρ_{xx} versus magnetic field (B) and antisymmetrization of the ρ_{xy} vs B data to remove mixings between ρ_{xx} and ρ_{xy} due to imperfect contact alignment. The carrier density was tuned through a bottom gate (Si substrate), where a gate voltage $V_g = 55 - 90\,\mathrm{V}$ was applied to tune the carrier density over the range explored in this study.

Figures 1 and 2 show the magnetoresistance (MR) and Hall effect data for our 55-nm-thick InSe sample 1 (all data presented in the main text are from sample 1 unless stated otherwise). In Fig. 1(a), we present the longitudinal MR data which exhibit WL behavior at low fields ($B < B_l = \hbar/4eD\tau \sim 2\,\mathrm{T}$ for our system with D as the diffusion constant) [21,44] and change into a negative paraboliclike MR at higher fields. The WL or WAL effects [45–47] are known to be induced by single-particle quantum interference corrections for electrons diffusing in a random impurity potential and lead to a negative (for WL) or positive (for WAL) MR [44,48,49] in the weak magnetic field limit ($\omega_C\tau \ll 1$), where ω_C is the cyclotron frequency ($\omega_C = eB/m^*$, where $m^* = 0.14m_e$ is the effective mass of electrons in InSe [15]) and τ is the momentum relaxation time. However, the crossover to a different type of negative MR above the critical field B_l as observed here is unusual compared to similar analyses performed in other 2D vdW materials [8,16].

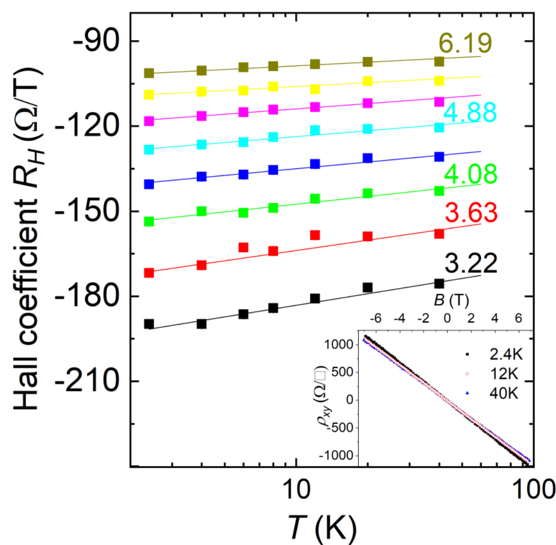

FIG. 2. Temperature dependence of Hall coefficient R_{H} at different electron densities (values marked on curves in units of $10^{12}/\mathrm{cm}^2$). Inset: Example transverse/Hall resistivity ρ_{xy} vs B data at different temperatures, plotted for $n = 3.63\times10^{12}/\,\mathrm{cm}^2$.

To further explore this negative parabolic MR behavior at $B > B_l$, we subtract the WL correction $\Delta\rho_{\mathrm{WL}}(B)$ which predominates at $B < B_l$. $\Delta\rho_{\mathrm{WL}}(B)$ is determined by fitting the low-field data ($B < 2\,\mathrm{T}$) to the Hikami-Larkin-Nagaoka (HLN) equation for 2D WL [48]. $\rho_{xx}\ (B) - \Delta\rho_{\mathrm{WL}}(B)\ - \rho_0$ is plotted in Fig. 1(b) with ρ_0 being the zero-field resistivity without the WL effect. A negative parabolic dependence is clearly observed. ρ_0 is obtained as the $B = 0$ intercept in fitting the high-field ($B > B_l$) data in Fig. 1(a) to a parabolic dependence. The temperature dependence of ρ_0 is shown in Fig. 1(c). Strikingly, it exhibits a logarithmic T dependence, even with the WL effect removed. This is a consequence of the EEI effect as discussed later. It is to be noted that, for back-gated multilayer InSe FETs, the electron wave function is confined to within ~5 nm of the InSe-$\mathrm{SiO_2}$ interface [37], justifying the formation of 2DEG and use of 2D transport equations in our study.

Figure 2 shows the T dependence of the Hall coefficient R_{H} extracted from a linear fit to ρ_{xy} vs B (shown in the inset). We observe a similar logarithmic behavior to this data as well. These data are clear signatures of the effect of EEIs for a 2D FL in our InSe system. In conventional semiconductor heterointerfaces, EEIs were found to give rise to a negative parabolic MR effect at magnetic fields where the Zeeman splitting effect is negligible [25,36], along with logarithmic corrections to the T dependence of zero-field conductance and the Hall coefficient [33,36]. While most prior transport studies on conventional semiconductor heterostructures and graphene are in the ballistic ($\frac{k_B T\tau}{\hbar} > 1$) and high-field ($\omega_C\tau > 1$) regime, the gated InSe nanoflake here resides in the

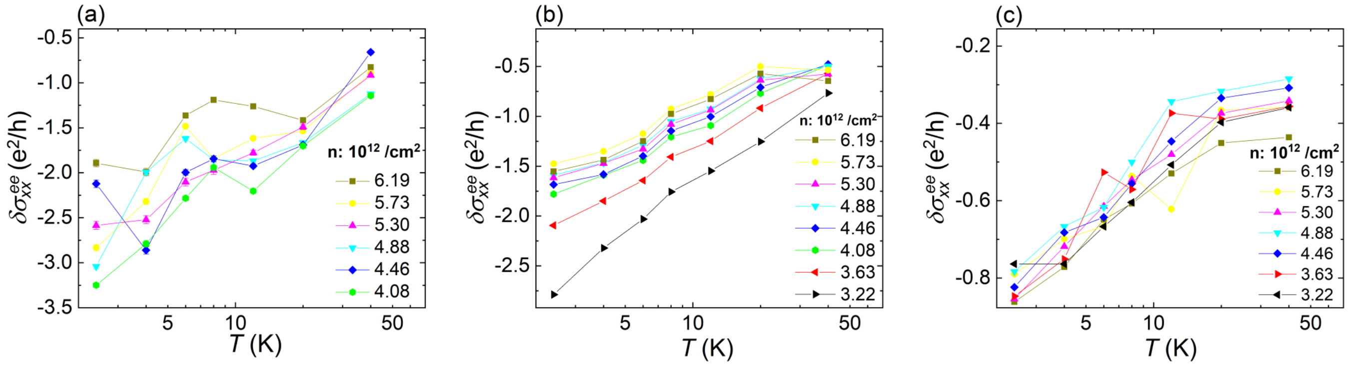

FIG. 3. EEI correction to Drude conductivity vs T, extracted from (a) negative parabolic MR (method 1); (b) zero-field resistance without the WL effect, given by ρ_0 (method 2); (c) change in Hall coefficient with temperature (method 3).

diffusive ($\frac{k_B T \tau}{\hbar} < 1$) and low-field ($\omega_C \tau < 1$) regime. From the Hall mobility (800 $\text{cm}^2/\text{V s}$ at 10 K—see the Supplemental Material, Sec. 1 [50]) of our system, we extract $\tau = 6 \times 10^{-14}$ s, which puts us in the diffusive regime for $T \lesssim 120$ K and in the low-field regime for $B \lesssim 12$ T.

Below, we outline three methods of extracting $\delta\sigma_{xx}^{ee}(T)$, the EEI correction to the Drude conductivity $\sigma_0 (= ne^2\tau/m^*)$, from these transport data.

The negative parabolic MR due to EEIs is given by [36]

$$\rho_{xx} = \frac{1}{\sigma_0}\left[1 - \frac{(1-(\omega_C\tau)^2)\delta\sigma_{xx}^{ee}}{\sigma_0}\right]. \tag{1}$$

In the weak-field limit ($\omega_C \tau \ll 1$), the correction to R_H is given by

$$\frac{\Delta R_\text{H}}{R_\text{H}^0} = -\frac{2\Delta\sigma_{xx}^{ee}}{\sigma_0}, \tag{2}$$

where R_H^0 is the classical Hall coefficient [33,36]. These relations are derived by inverting the 2D conductivity tensor $\boldsymbol{\sigma}$ with the corresponding EEI corrections added (Supplemental Material, Sec. 3 [50]), which are in turn derived by treating EEIs as first-order Coulomb interaction contributions to $\boldsymbol{\sigma}$ for a disordered 2DEG in the diffusive regime ($\tau < \frac{\hbar}{k_B T}$) [36]. For FL theory in the diffusive limit, $\delta\sigma_{xx}^{ee}(T)$ is known to have a logarithmic T dependence given by

$$\delta\sigma_{xx}^{ee} = \frac{e^2}{2\pi^2\hbar} f\left(F_0^\sigma\right) \ln\left(\frac{T}{T_0}\right), \tag{3}$$

where $T < T_0 = \frac{\hbar}{k_B \tau}$ and $f(F_0^\sigma) = 1 + 3[1 - \ln(1 + F_0^\sigma)/F_0^\sigma]$ [51,52].

We can extract $\delta\sigma_{xx}^{ee}(T)$ from fitting the data in Fig. 1(b) to the B^2 dependence according to Eq. (1) (method 1), or comparing $\rho_0(T)$ shown in Fig. 1(c) to the $B = 0$ limit of Eq. (1) (method 2), or fitting the Hall coefficient data shown in Fig. 2 to Eq. (2) (method 3). The results of these methods are shown in Fig. 3. From the extracted $\delta\sigma_{xx}^{ee}(T)$, we observe a logarithmic divergence as T is lowered in all three methods, as expected from Eq. (3). This provides further evidence for the EEI source of these corrections. It is also noted that $\delta\sigma_{xx}^{ee}(T)$ extracted from method 1 is not dependent on τ, while the $\delta\sigma_{xx}^{ee}(T)$ from method 2 is (Supplemental Material, Sec. 3 [50]). Therefore, the similarity in values and trend of $\delta\sigma_{xx}^{ee}(T)$ extracted from both methods 1 and 2 [Figs. 3(a) and 3(b)] indicates that the temperature dependence of τ (or the Drude conductivity) is not significant over this temperature range.

We can then use the logarithmic dependence of $\delta\sigma_{xx}^{ee}(T)$ to extract the FL parameter F_0^σ from Eq. (3). The results are plotted in Fig. 4. It is important to note that, even though the orders of magnitude of the corrections and the T dependence are consistent across all three methods, we observe an approximate factor of 3 higher magnitude in the $\delta\sigma_{xx}^{ee}(T)$ extracted from MR (methods 1 and 2) compared to the Hall coefficient analysis (method 3). This enhancement is also reflected in their larger slope of logarithmic $\delta\sigma_{xx}^{ee}(T)$ (Supplemental Material, Sec. 4 [50]), which is the relevant quantity for determining the FL parameter F_0^σ. Even though the difference in the slope of $\delta\sigma_{xx}^{ee}(T)$ is mostly within a factor of 3 across all methods, this difference becomes significant when extracting F_0^σ, due to the highly nonlinear dependence of the logarithmic slope of $\delta\sigma_{xx}^{ee}(T)$ on F_0^σ (Supplemental Material, Sec. 4 [50]). Next, we discuss the extracted F_0^σ from all three methods and compare to FL theory. We observe that F_0^σ extracted from the Hall effect using method 3 (Fig. 4)

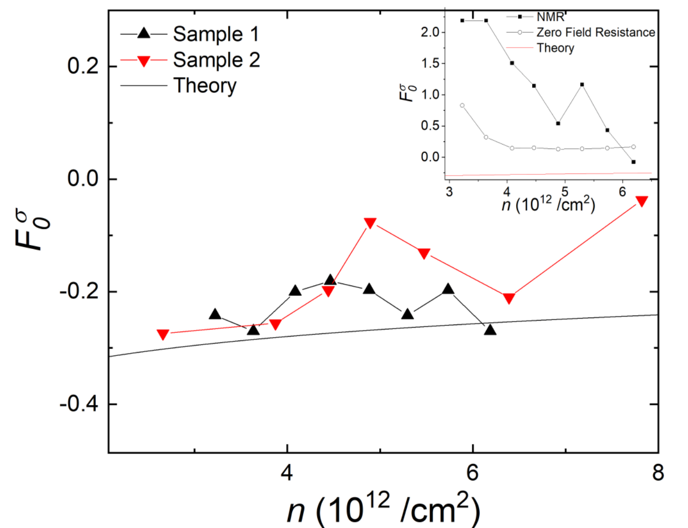

FIG. 4. FL parameter extracted using the Hall coefficient (method 3) plotted vs electron density. The solid line corresponds to the prediction of FL theory [Eq. (4)]. Inset: FL parameter extracted using methods 1 and 2 (for sample 1) vs electron density.

shows agreement with predictions of FL theory [51],

$$F_0^\sigma = -\frac{1}{2\pi}\left(\frac{r_s}{\sqrt{2-r_s^2}}\right)\ln\left[\frac{\sqrt{2}+\sqrt{2-r_s^2}}{\sqrt{2}-\sqrt{2-r_s^2}}\right], \quad (4)$$

where $r_s = 1/\sqrt{\pi(a_B^*)^2 n}$ is the 2D interaction parameter with a_B as the effective Bohr radius and n being the electron density. This prediction is valid for $r_s^2 < 2$, and we find that our system satisfies this inequality in the density range considered.

While F_0^σ extracted from Hall effect agrees with FL theory, F_0^σ extracted from MR data (methods 1 and 2) shows strong density dependences not consistent with FL theory (inset of Fig. 4). A possible reason for the observed discrepancy in F_0^σ extracted from MR, which is reflected in the higher $\delta\sigma_{xx}^{ee}(T)$ extracted from MR, may be the nonuniform current flow in the van der Pauw geometry, leading to errors in determining the exact ρ_{xx} of our sample. Even though we averaged our measurements across different contact configurations, and accounted for observed anisotropies in resistance between different contact configurations (according to Ref. [43]), errors due to the finite size of the contacts and the nonideal sample shape would still possibly lead to further deviations from the ideal van der Pauw resistance prefactor of $\pi/Ln(2)$ [43]. Further investigation is required to resolve this discrepancy.

It is also possible that other known effects contribute to negative MR but it is unlikely that these effects are relevant to InSe in this transport regime. In electronic systems with a high carrier mobility, the parabolic negative MR is complemented by a classical contribution, at strong magnetic fields. The presence of an external magnetic field allows electrons to become localized around impurities [53,54]. However, the relevance of this effect in here can be neglected considering the carrier mobility values ($\sim$1000 cm^2/V s at 10 K) of the system. The Kondo effect which explains the scattering of conduction electrons due to magnetic impurities can also lead to negative MR [55,56], but InSe is not expected to be magnetic [57] and the T-dependent resistivity here does not fully agree with the low-T upturn and saturation of resistivity, as in the Kondo effect. The chiral anomaly in Dirac/Weyl semimetals can also cause negative MR, where the application of $E||B$ breaks the chiral symmetry, and as a consequence, the conservation of chiral charge density is violated by a quantity called the anomaly term [58,59]. But this effect is inapplicable to InSe, a semiconductor.

In summary, we observe a negative parabolic MR effect in exfoliated InSe nanoflakes. We attribute this MR to EEI effects, as supported by the concomitant observation of a logarithmic T-dependent conductivity and Hall coefficient. We extract the EEI correction to Drude conductivity and the FL parameter F_0^σ within the framework of FL theory in the diffusive transport regime. We find that F_0^σ extracted from the Hall effect shows good agreement over the density range $(3-8\times10^{12}/\text{cm}^2)$ to FL theory. Our study shows the possibility of using InSe and other 2D semiconductors and heterostructures as a platform for studying 2D electron interaction physics in general.

X.P.A.G. acknowledges the financial support from NSF (DMR-1607631). F.C.C. and R.S. acknowledge funding support from the Ministry of Science and Technology (108-2622-8-002-016 and 108-2112-M-001-049-MY2), from the Ministry of Education in Taiwan (AI-MAT 108L900903), and from the Academia Sinica (AS-iMATE-108-11).

[1] K. S. Novoselov, A. K. Geim, S. V. Morozov, D. Jiang, Y. Zhang, S. V. Dubonos, I. V. Grigorieva, and A. A. Firsov, Science **306**, 666 (2004).

[2] A. K. Geim and K. S. Novoselov, Nat. Mater. **6**, 183 (2007).

[3] A. H. Castro Neto, F. Guinea, N. M. R. Peres, K. S. Novoselov, and A. K. Geim, Rev. Mod. Phys. **81**, 109 (2009).

[4] Z. Fei, T. Palomaki, S. Wu, W. Zhao, X. Cai, B. Sun, P. Nguyen, J. Finney, X. Xu, and D. H. Cobden, Nat. Phys. **13**, 677 (2017).

[5] S. Wu, V. Fatemi, Q. D. Gibson, K. Watanabe, T. Taniguchi, R. J. Cava, and P. Jarillo-Herrero, Science **359**, 76 (2018).

[6] E. Sajadi, T. Palomaki, Z. Fei, W. Zhao, P. Bement, C. Olsen, S. Luescher, X. Xu, J. A. Folk, and D. H. Cobden, Science **362**, 922 (2018).

[7] V. Fatemi, S. Wu, Y. Cao, L. Bretheau, Q. D. Gibson, K. Watanabe, T. Taniguchi, R. J. Cava, and P. Jarillo-Herrero, Science **362**, 926 (2018).

[8] H. Yuan, M. S. Bahramy, K. Morimoto, S. Wu, K. Nomura, B. J. Yang, H. Shimotani, R. Suzuki, M. Toh, C. Kloc, X. Xu, R. Arita, N. Nagaosa, and Y. Iwasa, Nat. Phys. **9**, 563 (2013).

[9] W. Han, R. K. Kawakami, M. Gmitra, and J. Fabian, Nat. Nanotechnol. **9**, 794 (2014).

[10] K. Premasiri and X. P. A. Gao, J. Phys.: Condens. Matter **31**, 193001 (2019).

[11] J. R. Schaibley, H. Yu, G. Clark, P. Rivera, J. S. Ross, K. L. Seyler, W. Yao, and X. Xu, Nat. Rev. Mater. **1**, 16055 (2016).

[12] X. Cui, G. H. Lee, Y. D. Kim, G. Arefe, P. Y. Huang, C. H. Lee, D. A. Chenet, X. Zhang, L. Wang, F. Ye, F. Pizzocchero, B. S. Jessen, K. Watanabe, T. Taniguchi, D. A. Muller, T. Low, P. Kim, and J. Hone, Nat. Nanotechnol. **10**, 534 (2015).

[13] L. Li, F. Yang, G. J. Ye, Z. Zhang, Z. Zhu, W. Lou, X. Zhou, L. Li, K. Watanabe, T. Taniguchi, K. Chang, Y. Wang, X. H. Chen, and Y. Zhang, Nat. Nanotechnol. **11**, 593 (2016).

[14] H. C. P. Movva, B. Fallahazad, K. Kim, S. Larentis, T. Taniguchi, K. Watanabe, S. K. Banerjee, and E. Tutuc, Phys. Rev. Lett. **118**, 247701 (2017).

[15] D. A. Bandurin, A. V. Tyurnina, G. L. Yu, A. Mishchenko, V. Zólyomi, S. V. Morozov, R. K. Kumar, R. V. Gorbachev, Z. R. Kudrynskyi, S. Pezzini, Z. D. Kovalyuk, U. Zeitler, K. S. Novoselov, A. Patanè, L. Eaves, I. V. Grigorieva, V. I. Fal'ko, A. K. Geim, and Y. Cao, Nat. Nanotechnol. **12**, 223 (2017).

[16] H. Schmidt, I. Yudhistira, L. Chu, A. H. Castro Neto, B. Özyilmaz, S. Adam, and G. Eda, Phys. Rev. Lett. **116**, 046803 (2016).

[17] F. Evers and A. D. Mirlin, Rev. Mod. Phys. **80**, 1355 (2008).

[18] P. A. Lee and T. V. Ramakrishnan, Rev. Mod. Phys. **57**, 287 (1985).

[19] B. Spivak, S. V. Kravchenko, S. A. Kivelson, and X. P. A. Gao, Rev. Mod. Phys. **82**, 1743 (2010).
[20] A. L. Efros and M. Pollak, *Electron-Electron Interactions in Disordered Systems* (Elsevier, Amsterdam, 1985).
[21] M. A. Paalanen, D. C. Tsui, and J. C. M. Hwang, Phys. Rev. Lett. **51**, 2226 (1983).
[22] B. J. F. Lin, M. A. Paalanen, A. C. Gossard, and D. C. Tsui, Phys. Rev. B **29**, 927 (1984).
[23] K. K. Choi, D. C. Tsui, and S. C. Palmateer, Phys. Rev. B **33**, 8216 (1986).
[24] V. T. Renard, I. V. Gornyi, O. A. Tkachenko, V. A. Tkachenko, Z. D. Kvon, E. B. Olshanetsky, A. I. Toropov, and J.-C. Portal, Phys. Rev. B **72**, 075313 (2005).
[25] L. Li, Y. Y. Proskuryakov, A. K. Savchenko, E. H. Linfield, and D. A. Ritchie, Phys. Rev. Lett. **90**, 076802 (2003).
[26] Y. Y. Proskuryakov, A. K. Savchenko, S. S. Safonov, M. Pepper, M. Y. Simmons, and D. A. Ritchie, Phys. Rev. Lett. **89**, 076406 (2002).
[27] J. L. Smith and P. J. Stiles, Phys. Rev. Lett. **29**, 102 (1972).
[28] A. A. Shashkin, S. V. Kravchenko, V. T. Dolgopolov, and T. M. Klapwijk, Phys. Rev. B **66**, 073303 (2002).
[29] N. N. Klimov, D. A. Knyazev, O. E. Omel'yanovskii, V. M. Pudalov, H. Kojima, and M. E. Gershenson, Phys. Rev. B **78**, 195308 (2008).
[30] A. Yu. Kuntsevich, L. A. Morgun, and V. M. Pudalov, Phys. Rev. B **87**, 205406 (2013).
[31] V. N. Kotov, B. Uchoa, V. M. Pereira, F. Guinea, and A. H. Castro Neto, Rev. Mod. Phys. **84**, 1067 (2012).
[32] J. Jobst, D. Waldmann, I. V. Gornyi, A. D. Mirlin, and H. B. Weber, Phys. Rev. Lett. **108**, 106601 (2012).
[33] C. W. Liu, C. Chuang, Y. Yang, R. E. Elmquist, Y. J. Ho, H. Y. Lee, and C. T. Liang, 2D Mater. **4**, 025007 (2017).
[34] G. M. Minkov, A. V. Germanenko, O. E. Rut, A. A. Sherstobitov, V. A. Larionova, A. K. Bakarov, and B. N. Zvonkov, Phys. Rev. B **74**, 045314 (2006).
[35] G. M. Minkov, O. E. Rut, A. V. Germanenko, A. A. Sherstobitov, V. I. Shashkin, O. I. Khrykin, and B. N. Zvonkov, Phys. Rev. B **67**, 205306 (2003).
[36] A. Houghton, J. R. Senna, and S. C. Ying, Phys. Rev. B **25**, 2196 (1982).
[37] K. Premasiri, S. K. Radha, S. Sucharitakul, U. R. Kumar, R. Sankar, F. C. Chou, Y. T. Chen, and X. P. A. Gao, Nano Lett. **18**, 4403 (2018).
[38] S. Sucharitakul, N. J. Goble, U. R. Kumar, R. Sankar, Z. A. Bogorad, F. C. Chou, Y. T. Chen, and X. P. A. Gao, Nano Lett. **15**, 3815 (2015).
[39] S. R. Tamalampudi, Y. Y. Lu, R. Kumar U., R. Sankar, C. D. Liao, K. Moorthy B., C. H. Cheng, F. C. Chou, and Y. T. Chen, Nano Lett. **14**, 2800 (2014).
[40] D. T. Do, S. D. Mahanti, and C. W. Lai, Sci. Rep. **5**, 17044 (2015).
[41] G. W. Mudd, S. A. Svatek, T. Ren, A. Patanè, O. Makarovsky, L. Eaves, P. H. Beton, Z. D. Kovalyuk, G. V. Lashkarev, Z. R. Kudrynskyi, and A. I. Dmitriev, Adv. Mater. **25**, 5714 (2013).
[42] S. Lei, L. Ge, S. Najmaei, A. George, R. Kappera, J. Lou, M. Chhowalla, H. Yamaguchi, G. Gupta, R. Vajtai, A. D. Mohite, and P. M. Ajayan, ACS Nano **8**, 1263 (2014).
[43] L. J. van der Pauw, Philips Res. Rep. **13**, 1 (1958).
[44] B. L. Altshuler, A. G. Aronov, and P. A. Lee, Phys. Rev. Lett. **44**, 1288 (1980).
[45] E. Abrahams, P. W. Anderson, D. C. Licciardello, and T. V. Ramakrishnan, Phys. Rev. Lett. **42**, 673 (1979).
[46] G. Bergmann, Phys. Rep. **107**, 1 (1984).
[47] S. Kawaji, Surf. Sci. **170**, 682 (1986).
[48] S. Hikami, A. I. Larkin, and Y. Nagaoka, Prog. Theor. Phys. **63**, 707 (1980).
[49] S. Chakravarty and A. Schmid, Phys. Rep. **140**, 193 (1986).
[50] See Supplemental Material at http://link.aps.org/supplemental/10.1103/PhysRevB.102.121301 for sample characterization, additional magnetoresistance and Hall effect data on samples 1 and 2, and further details on the determination of $\delta\sigma_{xx}^{ee}$ and F_0^σ from data.
[51] G. Zala, B. N. Narozhny, and I. L. Aleiner, Phys. Rev. B **64**, 214204 (2001).
[52] B. L. Altshuler and A. G. Aronov, Solid State Commun. **46**, 429 (1983).
[53] A. Dmitriev, M. Dyakonov, and R. Jullien, Phys. Rev. B **64**, 233321 (2001).
[54] A. D. Mirlin, D. G. Polyakov, F. Evers, and P. Wölfle, Phys. Rev. Lett. **87**, 126805 (2001).
[55] J. Kondo, Prog. Theor. Phys. **32**, 37 (1964).
[56] J. H. Chen, L. Li, W. G. Cullen, E. D. Williams, and M. S. Fuhrer, Nat. Phys. **7**, 535 (2011).
[57] T. Wang, J. Li, H. Jin, and Y. Wei, Phys. Chem. Chem. Phys. **20**, 7532 (2018).
[58] A. Juyal, A. Agarwal, and S. Mukhopadhyay, Phys. Rev. Lett. **120**, 096801 (2018).
[59] S. Liang, J. Lin, S. Kushwaha, J. Xing, N. Ni, R. J. Cava, and N. P. Ong, Phys. Rev. X **8**, 031002 (2018).